JOURNAL OF AGRICULTURAL AND FOOD CHEMISTRY

ARTICLE

pubs.acs.org/JAFC

Identification of Benzophenone *C*-Glucosides from Mango Tree Leaves and Their Inhibitory Effect on Triglyceride Accumulation in 3T3-L1 Adipocytes

Yi Zhang,[‡] Qian Qian,[§] Dandan Ge,[§] Yuhong Li,[⊥] Xinrui Wang,[⊥] Qiu Chen,[§] Xiumei Gao,[‡,⊥] and Tao Wang*[,‡]

[‡]Tianjin State Key Laboratory of Modern Chinese Medicine, 312 Anshanxi Road, Nankai District, Tianjin 300193, China

[§]Institute of Traditional Chinese Medicine, Tianjin University of Traditional Chinese Medicine, 312 Anshanxi Road, Nankai District, Tianjin 300193, China

[⊥]Key Laboratory of Pharmacology of Traditional Chinese Medical Formulae (Tianjin University of Traditional Chinese Medicine), Ministry of Education, 312 Anshanxi Road, Nankai District, Tianjin 300193, China

ABSTRACT: A 70% ethanol−water extract from the leaves of *Mangifera indica* L. (Anacardiaceae) inhibited triglyceride (TG) accumulation in 3T3-L1 cells. From the active fraction, seven new benzophenone *C*-glycosides, foliamangiferosides A (**1**), A_1 (**2**), A_2 (**3**), B (**4**), C_1 (**5**), C_2 (**6**), and C_3 (**7**), together with five known compounds were isolated and the structures were elucidated on the basis of chemical and physicochemical evidence. The effects of these compounds on TG and the free fatty acid level in 3T3-L1 cells were determined, and the structure−activity relationship was discussed. On the basis of the AMPK signaling pathway, several compounds were found to increase the AMPK enzyme expression and down-regulate lipogenic enzyme gene expression such as SREBP1c, FAS, and HSL.

KEYWORDS: *Mangifera indica*, AMPK signaling pathway, TG accumulation, 3T3-L1 cells, lipogenic enzyme gene expression

INTRODUCTION

The AMP-activated protein kinase (AMPK) signaling pathway plays an important role in regulating adipose mass, obesity, and diabetes. AMPK is a heterotrimeric protein containing an α catalytic subunit and β and γ regulatory subunits. It acts as a switch in regulating the balance of energy metabolism.[1] When the intracellular adenosine triphosphate concentration decreases and the AMP concentration increases in response to nutrient deprivation and pathological stresses, AMPK is activated by upstream kinases, including Ca^{2+} calmodulin-dependent protein kinase kinase β (CAMKKβ), LKB1, and TGF-β-activated kinase-1 (Tak1), resulting in phosphorylation of Thr172 on the α subunit followed by reduced energy storage and increased energy production to reestablish normal cellular energy balance.[2] AMPK activation leads to numerous metabolic changes that would be attractive targets in the treatment of metabolic disorders such as obesity, type-2 diabetes, and metabolic syndrome.

The effects of AMPK activation are pleiotropic in metabolically relevant tissues, such as the liver, skeletal muscle, adipose tissue, and the hypothalamus. AMPK is also directly activated by other indirect activators such as adiponectin, leptin, and interleukin-6.[3,4] Certain natural products have been found to have effects on AMPK activation. Berberine, an isoquinoline alkaloid isolated from *Rhizoma coptidis*, has been shown to increase GLUT4 translocation in L6 cells in a phosphatidylinositol 3-kinase-independent manner and reduce lipid accumulation in 3T3-L1 adipocytes. Resveratrol, a natural stilbene compound found in the skins of red grapes, and its analogues were found to have a stimulating effect on AMPK, and the lipid-lowering effect of polyphenols depend on SIRT1 activity.[5,6]

Mangoes belong to the genus *Mangifera*, consisting of numerous species of tropical fruit trees in the family Anacardiaceae. The mango tree (*Mangifera indica* L.) is a perennial woody plant widely distributed in the south of China (e.g., Yunnan, Guangxi, Guizhou, and Zhejiang provinces). The leaves of *M. indica* have been used as an antitussive in certain Chinese regions such as Guangxi province.[7] Several xanthone *C*-glycosides, such as mangiferin, gallotannins, and benzophenones, have previously been isolated from them.[8−10] However, the pharmacological research to date has only focused on the main constituent, mangiferin, which has been reported to have antidiabetic,[11] antiulcerogenic action,[12] and antimicrobial activity.[13]

During the course of our studies on bioactive constituents from Chinese natural medicines, we found that the 70% EtOH extract of the *M. indica* leaves showed a strong triglyceride (TG) accumulation inhibitory effect on the 3T3-L1 preadipocyte, which has served as a well-established in vitro model to assess adipogenesis and energy metabolism (see Chart 1). From the active fraction of mango leaves, seven new benzophenone *C*-glycosides, foliamangiferosides A (**1**), A_1 (**2**), A_2 (**3**), B (**4**), C_1 (**5**), C_2 (**6**), and C_3 (**7**), together with five known compounds,[14] iriflophenone-3-*C*-β-glucoside (**8**), iriflophenone-3-*C*-(2-*O*-*p*-hydroxybenzoyl)-β-D-glucopyranoside (**9**), maclurin-3-*C*-β-D-glucoside (**10**), 2,4′,6-trihydroxy-4-methoxybenzophenone-2-*O*-β-D-glucopyranoside (**11**),

Received: July 15, 2011
Accepted: September 18, 2011
Revised: September 17, 2011
Published: September 18, 2011

Chart 1. Structures of Compounds Isolated from *M. indica* Leaves

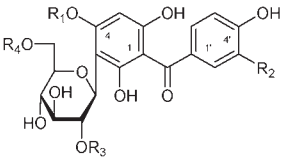

	R_1	R_2	R_3	R_4
Foliamangiferoside A (**1**):	CH_3	H	H	H
Foliamangiferoside A_1 (**2**):	CH_3	H	*(a)*	H
Foliamangiferoside A_2 (**3**):	CH_3	H	H	*(a)*
Foliamangiferoside B (**4**):	CH_3	OCH_3	H	H
Foliamangiferoside C_1 (**5**):	H	H	H	*(a)*
Foliamangiferoside C_2 (**6**):	H	H	*(a)*	*(a)*
Foliamangiferoside C_3 (**7**):	H	H	H	*(b)*

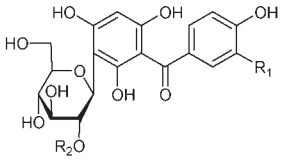

	R_1	R_2
8	H	H
9	H	*(a)*
10	OH	H

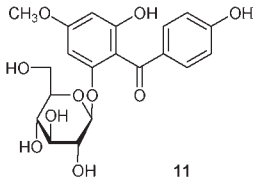

11

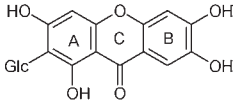

Mangiferin (**12**)

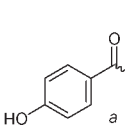

a

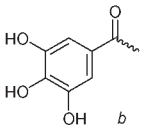

b

Glc: β-D-glucopyranosyl

and mangiferin (**12**) were obtained. Some of these increased AMPK activity and reduced lipid mass in adipocytes.

MATERIALS AND METHODS

General Procedures. The following instruments were used to obtain physical data: Optical rotations were measured on a Rudolph Autopol IV automatic polarimeter (l = 50 mm), IR were recorded on a Varian 640-IR FT-IR spectrophotometer, and UV spectra were recorded on a Varian Cary 50 UV−vis spectrophotometer. ^{1}H and ^{13}C NMR spectra were determined on a Varian 400MR spectrometer at 400 MHz for ^{1}H and 100 MHz for ^{13}C NMR, with tetramethylsilane (TMS) as an internal standard. Positive- and negative-ion HR-ESI-TOF-MS were recorded on an Agilent Technologies 6520 Accurate-Mass Q-Tof LC/MS spectrometer.

A highly porous synthetic resin (D101) was purchased from Haiguang Chemical Co., Ltd. (Tianjin, China). Silica gel CC were obtained from Qingdao Haiyang Chemical Co., Ltd. (48−75 μm, Qingdao, China). Sephadex LH-20 (Ge Healthcare Bio-Sciences, Swiss) was used to purify the total flavonoids from the whole residue. HPLC was performed on ODS (Cosmosil 5C18-MS-II, Tokyo, Japan; ∅ = 20 mm, L = 250 mm, flow rate: 9.0 mL/min), and the eluate was monitored with a UV detector (Shimadzu RID-10A UV−vis, Japan). Precoated TLC plates with silica gel GF_{254} (Tianjin Silida Technology Co., Ltd., Tianjin, China) were used to detect the purity of isolate achieved by spraying with 10% aqueous H_2SO_4−EtOH, following by heating.

Plant Material. In the present study, mango leaves were collected from Zhejiang Province, China, and identified by Dr. Tianxiang Li at Tianjin University of TCM as *Mangifera indica* L. The voucher specimen was deposited at the Academy of traditional Chinese Medicine of Tianjin University of TCM.

Extraction and Isolation of New Compounds 1−7. The dried leaves of *M. indica* L. were finely cut and extracted with 70% ethanol−water under reflux. Evaporation of the solvent under reduced pressure provided a 70% ethanol−water extract (23.26%). The 70% ethanol−water extract was partitioned into an EtOAc−H_2O (1:1, v/v) mixture to furnish an EtOAc-soluble fraction (6.51%) and an aqueous phase. A 4/5 volume of the aqueous phase was concentrated to 2 L under reduced pressure to give a concentrate, which was further centrifuged at 4000 rpm to furnish a supernatant. The supernatant was further subjected to D101 resin column chromatography (H_2O → 95% EtOH) to give the water- and 95% EtOH-eluted fractions (6.40% and 4.14%, respectively). The 95% EtOH-eluted fraction (72 g) was subjected to ordinary-phase silica gel column chromatography [$CHCl_3$−MeOH (10:1 → 5:1, v/v) → $CHCl_3$−MeOH−H_2O (7:3:1 → 6:4:1, v/v/v, lower layer) → MeOH] to give nine fractions [Fr. 1 (0.5 g), Fr. 2 (0.8 g), Fr. 3 (0.6 g), Fr. 4 (0.7 g), Fr. 5 (1.0 g), Fr. 6 (9.0 g), Fr. 7 (34.8 g), Fr. 8 (4.9 g), Fr. 9 (14.2 g)]. Fraction 6 (7.0 g) was separated by reversed-phase silica gel column chromatography [120 g, MeOH−H_2O (10:90 → 20:80 → 30:70 → 40:60 → 50:50 → 100:0, v/v)] to give seven fractions [Fr. 6-1 (0.1 g), Fr. 6-2 (4.9 g), Fr. 6-3 (0.2 g), Fr. 6-4 (0.6 g), Fr. 6-5 (0.4 g), Fr. 6-6 (0.4 g), Fr. 6-7 (0.2 g)]. Fraction 6-2 (4.9 g) was identified as foliamangiferoside A (**1**, 0.36%). Fraction 6-3 (0.2 g) was further purified by HPLC [MeOH−H_2O (20:80, v/v) + 1% HAc] to furnish foliamangiferosides A (**1**, 117.0 mg, 0.0087%), and B (**2**, 25.0 mg, 0.0018%). Fraction 6-4 (0.6 g) was subjected to HPLC [MeOH−H_2O (30:70, v/v) + 1% HAc] and further HPLC [MeOH−H_2O (20:80, v/v)] to afford foliamangiferoside B (**4**, 5.4 mg, 0.00040%).

The EtOAc layer (120.0 g) was subjected to SiO_2 gel column chromatography [$CHCl_3$ → $CHCl_3$−MeOH (100:1 → 5:1, v/v) → MeOH] to furnish seven fractions [Fr. 1 (0.8 g), Fr. 2 (2.2 g), Fr. 3 (1.0 g), Fr. 4 (0.5 g), Fr. 5 (0.2 g), Fr. 6 (73.0 g), Fr. 7 (46.0 g)]. Fraction 6 (60.0 g) was further separated by SiO_2 gel column chromatography [$CHCl_3$−MeOH (100:1 → 100:3 → 100:4 → 100:7 → 10:1, v/v) → MeOH], and eight fractions [Fr. 6-1 (0.1 g), Fr. 6-2 (10.4 g), Fr. 6-3 (1.3 g), Fr. 6-4 (3.4 g), Fr. 6-5 (2.7 g), Fr. 6-6 (0.7 g), Fr. 6-7 (6.8 g), Fr. 6-8 (30.5 g)] were obtained. Fr. 6-7 (5.0 g) was isolated with reversed-phase silica gel column chromatography [MeOH−H_2O (0:100 → 10:90 → 30:70 → 50:50 → 70:30 → 80:20 → 90:10 → 100:0, v/v)] to give seven fractions [Fr. 6-7-1 (379.2 mg), Fr. 6-7-2 (240.0 mg), Fr. 6-7-3 (893.5 mg), Fr. 6-7-4 (333.9 mg), Fr. 6-7-5 (382.2 mg), Fr. 6-7-6 (158.6 mg), Fr. 6-7-7 (100.9 mg), Fr. 6-7-8 (136.3 mg), Fr. 6-7-9 (115.0 mg), Fr. 6-7-10 (1720.8 mg)]. Fraction 6-7-3 (893.5 mg) was purified by HPLC [MeOH−H_2O (45:55, v/v) + 1% HAc] and further [MeOH−H_2O (40:60, v/v) + 1% HAc] to afford foliamangiferoside A_1 (**2**, 172.0 mg, 0.0154%). Fraction 6-7-5 (382.2 mg) was subjected to HPLC [MeOH−H_2O (50:50, v/v) +1% HAc] to give foliamangiferoside A_2 (**3**, 53.0 mg, 0.0047%), foliamangiferoside C_2 (**6**, 123.1 mg, 0.0110%). Fraction 6-8 (25.0 g) was subjected to normal-phase silica gel column chromatography [$CHCl_3$−MeOH−H_2O (10:3:1 → 7:3:1, v/v/v, lower layer) → MeOH] to afford seven fractions [Fr. 6-8-1 (0.3 g), Fr. 6-8-2 (1.1 g), Fr. 6-8-3 (2.6 g), Fr. 6-8-4 (5.5 g), Fr. 6-8-5 (6.7 g), Fr. 6-8-6 (0.7 g), Fr. 6-8-7 (6.5 g)]. Fraction 6-8-2 (1.1 g) was fractionated by Sephadex LH-20 column chromatography (MeOH) and further HPLC [MeOH−H_2O (45:55, v/v) + 1% HAc] to give foliamangiferoside A_1 (**2**, 7.3 mg, 0.0011%). Fraction 6-8-3 (1.7 g) was purified by Sephadex LH-20 column chromatography (MeOH) to give six fractions [Fr. 6-8-3-1 (13.0 mg), Fr. 6-8-3-2 (498.3 mg), Fr. 6-8-3-3 (182.3 mg), Fr. 6-8-3-4

Table 1. ^{13}C NMR (100 MHz) Data of Compounds 1−7

	1[a]	1[b]	2[a]	3[a]	4[a]	4[b]	5[a]	6[a]	7[a]
1	108.9	108.8	109.1	108.5	109.1	108.9	107.1	107.5	107.1
2	159.6	155.5	158.5	159.6	159.2	155.6	161.2	161.3	161.5
3	105.4	104.3	103.4	105.3	105.5	104.5	104.2	102.6	104.2
4	163.4	159.3	161.6	163.6	163.3	159.4	162.8	161.4	163.0
5	92.4	91.1	91.9	92.5	92.5	91.3	96.4	95.8	96.5
6	160.5	156.2	160.2	160.9	160.4	156.4	161.0	162.5	160.8
7	198.4	193.6	198.0	198.4	198.2	193.6	198.9	198.9	199.0
1′	132.5	130.0	132.3	132.7	132.7	130.2	133.1	133.1	133.1
2′	133.1	131.5	133.3	133.0	113.3	111.5	132.8	132.9	132.8
3′	115.7	114.7	115.7	115.6	148.6	147.3	115.5	115.4	115.5
4′	163.4	161.7	163.1	163.1	153.0	151.6	162.6	162.6	162.7
5′	115.7	114.7	115.7	115.6	115.5	114.6	115.5	115.4	115.5
6′	133.1	131.5	133.3	133.0	126.3	124.9	132.8	132.9	132.8
1″	76.3	74.4	74.5	76.4	76.4	74.6	76.6	74.6	76.7
2″	73.3	71.6	74.2	73.4	73.5	71.8	73.7	74.3	73.6
3″	79.8	77.9	77.1	79.4	79.8	78.1	79.3	77.2	79.6
4″	71.5	69.2	71.1	71.3	71.5	69.4	71.2	71.4	71.5
5″	82.5	80.8	82.5	79.6	82.6	81.0	79.5	79.9	79.9
6″	62.4	60.1	61.9	64.3	62.5	60.2	64.3	64.3	64.9
4-OCH$_3$	56.3	55.4	56.1	56.2	56.5	55.5			
3′-OCH$_3$					56.3	55.5			
1‴			122.0	121.9			121.8	122.2	121.2
2‴			132.8	132.8			132.8	133.0	110.2
3‴			115.9	116.2			116.2	115.9	146.4
4‴			163.1	163.4			163.3	163.2	139.8
5‴			115.9	116.2			116.2	115.9	146.4
6‴			132.8	132.8			132.8	133.0	110.2
7‴			166.9	168.0			168.1	167.4	168.4
1⁗								121.8	
2⁗								132.9	
3⁗								116.2	
4⁗								163.4	
5⁗								116.2	
6⁗								132.9	
7⁗								168.1	

[a] In CD$_3$OD. [b] In DMSO-d_6.

(348.5 mg), Fr. 6-8-3-5 (514.8 mg), Fr. 6-8-3-6 (62.3 mg)]. Fraction 6-8-3-4 (348.5 mg) was further purified by HPLC [MeOH−H$_2$O (40:60, v/v) + 1% HAc] to afford foliamangiferoside A$_1$ (**2**, 95.3 mg, 0.0120%). Fraction 6-8-5 (5.0 g) was subjected to Sephadex LH-20 column chromatography [MeOH] to give five fractions [Fr. 6-8-5-1 (373.3 mg), Fr. 6-8-5-2 (2183.8 mg), Fr. 6-8-5-3 (2071.2 mg), Fr. 6-8-5-4 (495.6 mg), Fr. 6-8-5-5 (47.3 mg)]. Fractions 6-8-5-2 (2183.8 mg) and 6-8-5-3 (2071.2 mg) were isolated by HPLC [MeOH−H$_2$O (40:60, v/v) +1% HAc] to give foliamangiferosides A (**1**, 95.5 mg, 0.0360%), and C$_1$ (**5**, 29.3 mg, 0.0103%) and C$_3$ (**7**, 100.3 mg, 0.0358%), respectively.

Foliamangiferoside A (1). A pale yellow powder. ^{1}H NMR (DMSO-d_6): δ_H 7.61 (2H, d, J = 8.4 Hz, H-2′,6′), 6.81 (2H, d, J = 8.4 Hz, H-3′,5′), 6.08 (1H, s, H-5), 4.64 (1H, d, J = 9.6 Hz, H-1″), 3.71 (3H, s, 4-OCH_3), [3.61 (1H, br d, ca. J = 11 Hz), 3.52 (1H, br d, ca. J = 11 Hz), H$_2$-6″], 3.51 (1H, m, H-2″), 3.24 (1H, m, H-3″), 3.22 (2H, m, overlapped, H-4″ and -5″). ^{1}H NMR (CD$_3$OD): δ_H 7.65 (2H, d, J = 6.8 Hz, H-2′,6′), 6.78 (2H, d, J = 6.8 Hz, H-3′,5′), 6.10 (1H, s, H-5), 4.85 (1H, d, J = 7.6 Hz, H-1″), 3.88 (1H, m, H-2″), 3.80 (3H, s, 4-OCH_3), [3.84 (1H, dd, J = 11.2, 5.6 Hz), 3.71 (1H, dd, J = 11.2, 3.6 Hz), H$_2$-6″], 3.45 (2H, m, H-3″,4″), 3.37 (1H, m, H-5″). ^{13}C NMR (DMSO-d_6 and CD$_3$OD): δ_C see Table 1. $[\alpha]^{25}_D$ −23.1° (c 1.08, MeOH). UV (MeOH) λ_{max} (log ε): 290 (4.16) nm. IR (KBr) ν_{max}: 3282, 2975, 2944, 2884, 1722, 1607, 1511, 1447, 1373, 1083, 1022, 945, 901, 847, 818 cm^{-1}. Positive-ion mode HR-Q-TOF-ESI-MS (m/z): [M + Na]$^+$ calcd for $C_{20}H_{22}O_{10}Na$, 445.1105; found 445.1103; Negative-ion mode HR-Q-TOF-ESI-MS (m/z): [M − H]$^-$ calcd for $C_{20}H_{21}O_{10}$ 421.1140; found 421.1144.

Foliamangiferoside A$_1$ (2). A pale yellow powder. ^{1}H NMR (CD$_3$OD): δ_H 7.82 (2H, d, J = 7.2 Hz, H-2‴,6‴), 7.76 (2H, d, J = 8.4 Hz, H-2′,6′), 6.82 (4H, br s, H-3′,5′ and -3‴,5‴), 5.85 (1H, s, H-5), 5.47 (1H, br s, H-2″), 5.17 (1H, d, J = 10.0 Hz, H-1″), [3.87 (1H, m), 3.80 (1H, m), H$_2$-6″], 3.83 (1H, m, H-3″), 3.65 (1H, dd, J = 8.8, 8.8 Hz, H-4″), 3.54 (1H, m, H-5″), 3.54 (3H, s, 4-OCH_3). ^{13}C NMR (CD$_3$OD): δ_C see Table 1. $[\alpha]^{25}_D$ −161.9° (c 1.20, MeOH). UV (MeOH) λ_{max} (log ε): 275 (4.23, shoulder), 260 (4.28). IR (KBr) ν_{max}: 3352, 2935, 2850, 1712, 1609, 1513, 1442, 1375, 1318, 1266, 1207, 1171, 1127, 1071, 1027, 949, 851, 815 cm^{-1}. Positive-ion mode HR-Q-TOF-ESI-MS (m/z): [M + Na]$^+$ calcd for $C_{27}H_{26}O_{12}Na$: 565.1316; found 565.1323; Negative-ion mode HR-Q-TOF-ESI-MS (m/z): [M − H]$^-$ calcd for $C_{27}H_{25}O_{12}$: 541.1351; found 541.1377.

Foliamangiferoside A$_2$ (3). A pale yellow powder. ^{1}H NMR (CD$_3$OD): δ_H 7.79 (2H, d, J = 8.4 Hz, H-2‴,6‴), 7.64 (2H, d, J = 8.4 Hz, H-2′,6′), 6.77 (2H, d, J = 8.8 Hz, H-3′,5′), 6.73 (2H, d, J = 8.8 Hz, H-3‴,5‴), 6.10 (1H, s, H-5), 4.94 (1H, d, J = 10.0 Hz, H-1″), [4.56 (1H, dd, J = 12.0, 4.0 Hz), 4.49 (1H, dd, J = 12.0, 2.0 Hz), H$_2$-6″], 3.90 (1H, dd, J = 10.4, 8.8 Hz, H-2″), 3.78 (3H, s, 4-OCH_3), 3.69 (1H, m, H-5″), 3.56 (1H, dd, J = 9.2, 9.2 Hz, H-4″), 3.51 (1H, dd, J = 8.8, 8.8 Hz, H-3″). ^{13}C NMR (CD$_3$OD): δ_C see Table 1. $[\alpha]^{25}_D$ −60.1° (c 1.71, MeOH). UV (MeOH) λ_{max} (log ε): 311 (4.05, shoulder), 260 (4.24). IR (KBr) ν_{max}: 3369, 2925, 1695, 1608, 1514, 1447, 1376, 1317, 1280, 1167, 1121, 1085, 1012, 943, 850, 816 cm^{-1}. Positive-ion mode HR-Q-TOF-ESI-MS (m/z): [M + Na]$^+$ calcd for $C_{27}H_{26}O_{12}Na$: 565.1316; found 565.1317; Negative-ion mode HR-Q-TOF-ESI-MS (m/z): [M − H]$^-$ calcd for $C_{27}H_{25}O_{12}$: 541.1351; found 541.1372.

Foliamangiferoside B (4). A pale yellow powder. ^{1}H NMR (DMSO-d_6): δ_H 7.35 (1H, br s, H-2′), 7.16 (1H, br d, ca. J = 8 Hz, H-6′), 6.79 (1H, d, J = 8.0 Hz, H-5′), 6.08 (1H, s, H-5), 4.63 (1H, d, J = 9.6 Hz, H-1″), 3.79 (3H, s, 3′-OCH_3), 3.70 (3H, s, 4-OCH_3), [3.60 (1H, br d, ca. J = 11 Hz), 3.53 (1H, m, overlapped), H$_2$-6″], 3.55 (1H, m, overlapped, H-2″), 3.21 (3H, m, overlapped, H-3″, 4″ and 5″). ^{1}H NMR (CD$_3$OD): δ_H 7.39 (1H, d, J = 2.0 Hz, H-2′), 7.28 (1H, dd, J = 8.0, 2.0 Hz, H-6′), 6.78 (1H, d, J = 8.0 Hz, H-5′), 6.10 (1H, s), 3.87 (3H, s, 3′-OCH_3), 4.85 (1H, d, J = 10.0 Hz, H-1″), 3.84 (1H, m, H-2″), [3.84 (1H, m), 3.70 (1H, dd, J = 12.0, 4.8 Hz), H-6″], 3.81 (3H, s, 4-OCH_3), 3.43 (1H, m, H-3″), 3.42 (1H, m, H-4″), 3.37 (1H, m, H-5″). ^{13}C NMR (CD$_3$OD): δ_C see Table 1. $[\alpha]^{25}_D$ −3.5° (c. 0.28, MeOH). UV (MeOH) λ_{max} (log ε): 315 (3.97), 284 (3.88, shoulder), 230 (4.22). IR (KBr) ν_{max}: 3373, 2927, 2860, 1705, 1622, 1591, 1515, 1456, 1428, 1373, 1287, 1210, 1166, 1121, 1084, 1029, 880, 816 cm^{-1}. Positive-ion mode HR-Q-TOF-ESI-MS (m/z): [M + Na]$^+$ calcd for $C_{21}H_{24}O_{11}Na$: 475.1211; found 475.1219; Negative-ion mode HR-Q-TOF-ESI-MS (m/z): [M − H]$^-$ calcd for $C_{21}H_{23}O_{11}$: 451.1246; found 451.1262.

Foliamangiferoside C$_1$ (5). A pale yellow powder. ^{1}H NMR (CD$_3$OD): δ_H 7.85 (2H, d, J = 8.4 Hz, H-2‴,6‴), 7.62 (2H, d, J = 8.4 Hz, H-2′,6′), 6.79 (4H, m, J = 8.4 Hz, H-3′,5′ and 3‴,5‴), 6.01 (1H, s, H-5), 5.00 (1H, d, J = 10.0 Hz, H-1″), [4.62 (1H, dd, J = 12.0, 3.2 Hz), 4.53 (1H, br d, ca. J = 12 Hz), H$_2$-6″], 3.97 (1H, dd, J = 9.2, 8.8 Hz, H-2″), 3.76 (1H, m, H-5″), 3.63 (1H, dd, J = 9.2, 9.2 Hz, H-4″), 3.59 (1H, dd, J = 9.2, 8.8 Hz, H-3″). ^{13}C NMR (CD$_3$OD): δ_C see Table 1. $[\alpha]^{25}_D$ −58.7° (c. 1.30, MeOH). UV (MeOH) λ_{max} (log ε): 315 (4.13), 260 (4.28). IR (KBr) ν_{max}: 3343, 2935, 2858, 1715, 1610, 1587, 1505, 1466, 1375, 1287, 1121, 1082, 890, 826 cm^{-1}. Positive-ion mode HR-Q-TOF-ESI-MS (m/z): [M + Na]$^+$ calcd for $C_{26}H_{24}O_{12}Na$: 551.1160;

Table 2. Gene-Specific Primers Used for Quantitative Real-Time RT-PCR

gene name	forward	reverse
SREBP 1c	5′-GCGCCATGGACGAGCTG-3′	5′-TTGGCACCTGGGCTGCT-3′
FAS	5′-ACAAACTGCACCCTGACCCAGA-3′	5′-TGCTGGTTGCTGTGCATGGCT-3′
AMPK	5′-AAGCCGACCCAATGACATCA-3′	5′-CTTCCTTCGTACACGCAAAT-3′
HSL	5′-TGAGATGGTAACTGTGAGCC-3′	5′-ACTGAGATTGAGGTGCTGTC-3′
GADPH	5′-AACTTTGGCATTGTGGAAGG-3′	5′-GGATGCAGGGATGATGTTCT-3′

found 551.1151; Negative-ion mode HR-Q-TOF-ESI-MS (m/z): $[M - H]^-$ calcd for $C_{26}H_{23}O_{12}$: 527.1195; found 527.1190.

Foliamangiferoside C_2 (6). A pale yellow powder. ^{1}H NMR (CD_3OD): δ_H 5.82 (1H, s, H-5), 7.86−7.61 (2H, m, H-2′,6′, -2‴,6‴, and -2⁗,6⁗), 6.78 (6H, m, H-3′,5′, -3‴,5‴, and -3⁗,5⁗), 5.59 (1H, dd, J = 8.8, 8.8 Hz, H-2″), 5.27 (1H, d, J = 10.0 Hz, H-1″), [4.66 (1H, dd, J = 12.0, 3.2 Hz), 4.58 (1H, m), H_2-6″], 3.87 (1H, m, H-3″), 3.86 (1H, br d, ca. J = 10 Hz, H-5″), 3.78 (1H, br d, ca. J = 9 Hz, H-4″). ^{13}C NMR (CD_3OD): δ_C see Table 1. $[\alpha]^{25}_D$ −167.1° (*c*. 1.61, MeOH). UV (MeOH) λ_{max} (log ε): 310 (4.12), 260 (4.53). IR (KBr) ν_{max}: 3333, 2945, 2865, 1710, 1605, 1578, 1500, 1464, 1355, 1290, 1127, 1085, 900, 856 cm^{-1}. Positive-ion mode HR-Q-TOF-ESI-MS (m/z): $[M + Na]^+$ calcd for $C_{34}H_{30}O_{14}Na$: 671.1371; found 671.1381; Negative-ion mode HR-Q-TOF-ESI-MS (m/z): $[M - H]^-$ calcd for $C_{34}H_{29}O_{14}$: 647.1406; found 647.1427.

Foliamangiferoside C_3 (7). A pale yellow powder. ^{1}H NMR (CD_3OD): δ_H 7.60 (2H, d, J = 8.8 Hz, H-2′,6′), 7.09 (2H, s, H-2‴,6‴), 6.77 (2H, d, J = 8.8 Hz, H-3′,5′), 5.98 (1H, s, H-5), 4.95 (1H, d, J = 10.0 Hz, H-1″), [4.58 (1H, dd, J = 12.0, 1.6 Hz), 4.46 (1H, dd, J = 12.0, 7.2 Hz), H_2-6″], 3.99 (1H, dd, J = 9.2, 9.2 Hz, H-2″), 3.73 (1H, m, H-5″), 3.62 (1H, dd, J = 9.2, 9.2 Hz, H-4″), 3.56 (1H, dd, J = 8.8, 8.8 Hz, H-3″). ^{13}C NMR (CD_3OD): δ_C see Table 1. $[\alpha]^{25}_D$ −23.0° (*c* 1.41, MeOH). UV (MeOH) λ_{max} (log ε): 285 (4.27). IR (KBr) ν_{max}: 3321, 2942, 2863, 1696, 1625, 1608, 1511, 1449, 1384, 1235, 1167, 1081, 1034, 848, 824 cm^{-1}. Positive-ion mode HR-Q-TOF-ESI-MS (m/z): $[M + Na]^+$ calcd for $C_{26}H_{24}O_{14}Na$: 583.1058; found 583.1059; Negative-ion mode HR-Q-TOF-ESI-MS (m/z): $[M - H]^-$ calcd for $C_{26}H_{23}O_{14}$: 559.1093; found 559.1109.

Bioassay. *3T3-L1 Cell Differentiation.* 3T3-L1 cells (Cell Resource Center, IBMS, CAMS/PUMC) were maintained in low-glucose Dulbecco's modified Eagle's medium (Thermo Scientific, West Palm Beach, FL) supplemented with 10% calf serum (Thermo Scientific). Confluent 3T3-L1 preadipocytes were induced to differentiate into adipocytes as literature.[15] Briefly, 1 day after confluence, the cells were treated with high-glucose Dulbecco's modified Eagle's medium containing 10% fetal bovine serum (Thermo Scientific), 1 μM dexamethasone (Sigma, St. Louis, MO), 0.5 mM 3-isobutyl-1-methylxanthine (Sigma), and 10 g/mL insulin (Sigma) for 3 days. At the same time, cells were treated with or without 30 μM sample DMSO solution (final DMSO concentration was 0.5%). Subsequently, cells were then switched to 10% FBS/DMEM media containing only 5 μg/mL insulin for 3 more days and then switched to 10% FBS/DMEM media without insulin. Differentiated cells were used when at least 95% of the cells showed an adipocyte phenotype by accumulation of lipid droplets.

Oil Red O Staining. Cells were washed twice with PBS and then fixed for 30 min with 10% formalin. Oil Red O stain (5% Oil Red O in 70% pyridine) was applied for 10 min, and cells were then washed three times with 70% ethanol. The lipid droplets in cells were stained with oil red O and observed under a light microscope.

Measurement of Lipolytic Activity. Confluent cultures of 3T3-L1 cells in 48-well plates (Costar) were induced as previously described. The amounts of intracellular triglycerides and nonesterified fatty acid (NEFA) were determined with the Triglycerides Kit (BioSino Biotechnology and Science Inc., China) and NEFA-C Kit (NEFA C-test wako, Japan) after cell lysis, respectively. TG and NEFA values were corrected on the basis of their protein content.

RNA Extraction and cDNA Synthesis. Confluent cultures of 3T3-L1 cells in six-well plates (Costar) were induced as previously described. Total RNA was isolated from 3T3-L1 adipocytes with TRIzol reagent (Invitrogen, Carlsbad, CA). One microgram of RNA was reverse transcribed by the High Capacity cDNA Reverse Transcription Kit (Applied Biosystems, Foster City, CA) to obtain cDNA according to the protocols provided by the manufacturer. Briefly, the total reaction volume was 20 μL with the reaction incubated as follows in an PE-480 HYBAID (Perkin-Elmer, Waltham, MA): 10 min at 25 °C, 120 min at 37 °C, 5 min at 85 °C, hold at 4 °C.

Real-Time PCR. Real-time PCR was performed with an Applied Biosystems 7500 Real-Time PCR System (Applied Biosystems) using Power SYBR Green PCR master mix (Applied Biosystems) according to the protocols provided by the manufacturer. Briefly, PCR was performed in a final volume of 20 μL including 10 ng of sample cDNA, 5 μM specific forward and reverse primers, and 10 μL of Power SYBR green PCR Master Mix. PCR reactions consisted of an initial denaturating cycle at 95 °C for 10 min, followed by 40 amplification cycles: 15 s at 95 °C and 1 min at 60 °C. The primers used were as Table 2. Results were presented as levels of expression relative to those of controls after normalization to GADPH using the $2^{-\Delta\Delta CT}$ method.[16] Analysis was carried out in triplicates.

Statistical Analysis. Values are expressed as mean ± SD. All the grouped data were statistically performed with SPSS 11.0. Significant differences between means were evaluated by one-way analysis of variance (ANOVA). $P < 0.05$ was considered to indicate statistical significance.

RESULTS AND DISCUSSION

Structures of Foliamangiferosides A (1), A_1 (2), A_2 (3), B (4), C_1 (5), C_2 (6), and C_3 (7). Foliamangiferoside A (**1**) was obtained as a pale yellow amorphous powder with negative optical rotation ($[\alpha]^{25}_D$ −23.1°, MeOH). Its IR spectrum showed absorptions due to hydroxyl (3282 cm^{-1}), unsaturated carboxyl (1722 cm^{-1}), and aromatic ring (1606, 1511, and 1447 cm^{-1}). The molecular formula $C_{20}H_{22}O_{10}$ of **1** was established on the basis of HR-Q-TOF-ESI-MS at m/z 421.1144 $[M - H]^-$ and 445.1103 $[M + Na]^+$, together with the ^{1}H and ^{13}C NMR spectra. The ^{13}C NMR spectrum (DMSO-d_6) (Table 1) showed twenty signals in total, among which six were assigned to a *C*-β-D-glucopyranosyl moiety (δ_C 80.8, 77.9, 74.4, 71.6, 69.2, 60.1),[17] and one was due to the methoxyl group [δ_C 56.3 (4-OCH_3)]. The remaining thirteen signals suggested the presence of a benzophenone or xanthone framework. The ^{1}H NMR (DMSO-d_6) spectrum of **1** showed signals assignable to a AA′BB′-system of aromatic protons [δ 7.61 (2H, d, J = 8.4 Hz, H-2′,6′), 6.81 (2H, d, J = 8.4 Hz, H-3′,5′)], an isolated aromatic proton at δ 6.08 (1H, s, H-5), and a *C*-β-D-glucopyranosyl part [4.64 (1H, d, J = 9.6 Hz), H-1″] together with one methoxyl group [δ 3.71 (3H, s, 4-OCH_3)]. In the HMBC experiment of **1**, a long-range correlation was observed between the δ_H 7.61 (H-2′,6′) and δ_C 193.6, δ_H 6.08

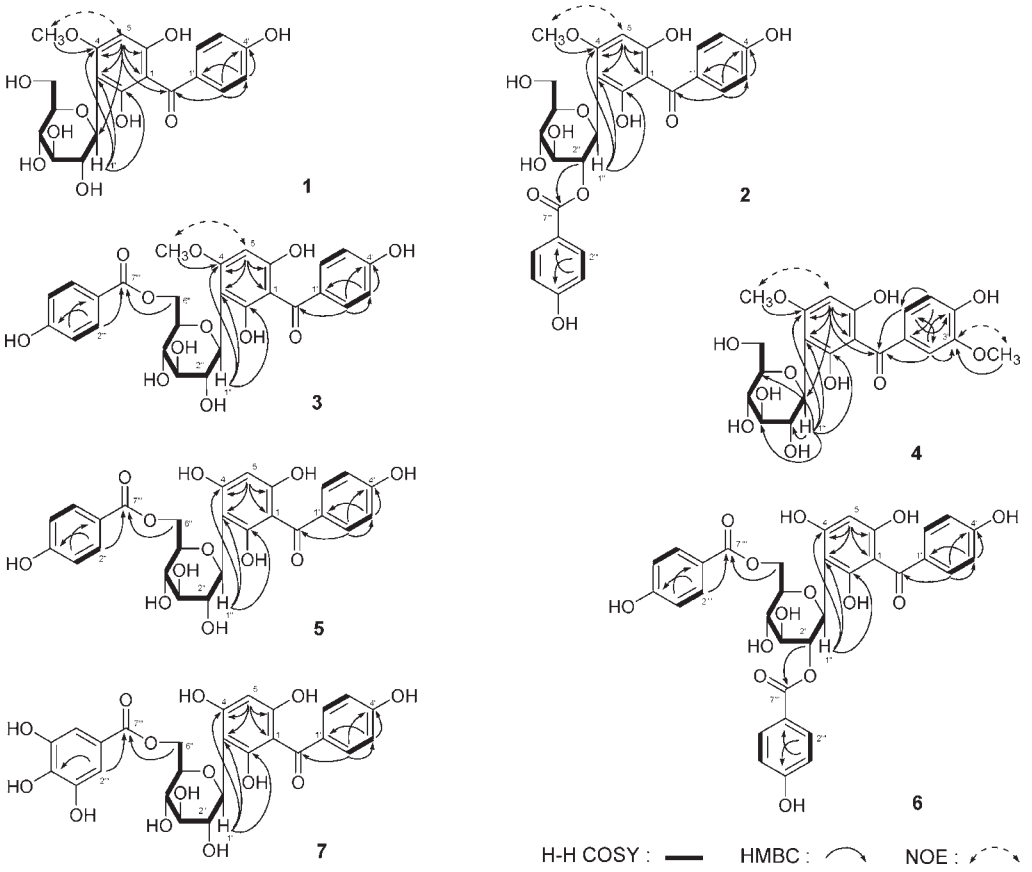

Figure 1. Key ^{1}H−^{1}H COSY, HMBC, and NOE correlations of compounds **1**−**7**.

(H-5) and δ_C 193.6 (*C*═O), 159.3 (C-4), 156.2 (C-6), 108.8 (C-1), and 104.3 (C-3), respectively. On the basis of the above-mentioned evidence, the benzophenone framework and the location of hydroxyl were revealed. Furthermore, the following long-range correlations in the HMBC experiment were observed, too: δ_H 4.64 (H-1″) and δ_C 155.5 (C-2), 104.3 (C-3), 159.3 (C-4); δ_H 3.71 (4-OC*H*$_3$) and δ_C 159.3 (C-4). Furthermore, in the NOESY experiment of **1** (Figure 1), an NOE correlation was observed between δ_H 3.71 (4-OC*H*$_3$) and δ_H 6.08 (H-5). Then the location of the methoxyl group and glucosyl C−C linkage was characterized as shown in Figure 1. Consequently, the structure of foliamangiferoside A (**1**) was elucidated to be 2,4′,6-trihydroxy-4-methoxybenzophenone-3-*C*-*β*-D-glucopyranoside.

Foliamangiferosides A$_1$ (**2**) and A$_2$ (**3**) were also isolated as pale yellow amorphous powders and both with negative optical rotations (**2**: $[\alpha]^{25}_D$ −161.9°; **3**: $[\alpha]^{25}_D$ −60.1°, both MeOH), respectively. The molecular formula, $C_{27}H_{26}O_{12}$, of them were determined from the HR-Q-TOF-ESI-MS positive-ion [**2**: *m*/*z* 565.1323 [M + Na]$^+$; **3**: 565.1317 [M + Na]$^+$] and negative ion [**2**: *m*/*z* 541.1377 [M − H]$^-$; **3**: 541.1372 [M − H]$^-$] measurement. The ^{1}H (CD_3OD), ^{13}C NMR (CD_3OD, Table 1) and various kinds of 2D NMR spectra including ^{1}H−^{1}H COSY, HMQC, HMBC, and NOESY (Figure 1) indicated that both of **2** and **3** had the same aglycon, 2,4′,6-trihydroxy-4-methoxybenzophenone as **1** {[**2**: (7.75−7.83 (2H, m, H-2′,6′), 6.74−6.83 (2H, m, H-3′,5′), 5.85 (1H, s, H-5), 3.54 (3H, s); δ_C 198.0 (C═O); [**3**: (7.64 (2H, d, *J* = 8.8 Hz, H-2′,6′), 6.77 (2H, d, *J* = 8.8 Hz, H-3′,5′), 6.10 (1H, s, H-5), 3.78 (3H, s); δ_C 198.4 (C═O)]}, a *C*-*β*-D-glucopyranosyl [**2**: 5.17 (1H, d, *J* = 10.0 Hz, H-1″); **3**: 4.94 (1H, d, *J* = 10.0 Hz, H-1″)], and both of the *C*-*β*-D-glucopyranosyls for **2** and **3** linked at the 3-position of the aglycon, which were determined with HMBC experiment. Futhermore, there was a *p*-hydroxybenzoyl group for both **2** [7.75−7.83 (2H, m, H-2‴,6‴), 6.74 (2H, m, H-3′,5′); δ_C 166.9 (C-7‴)] and **3** [7.79 (2H, d, *J* = 8.8 Hz, H-2‴,6‴), 6.73 (2H, d, *J* = 8.8 Hz, H-3‴,5‴); δ_C 168.0 (C-7‴)]. In the ^{1}H−^{1}H COSY experiment on **2**, proton correlations were observed between δ_H 5.17 (H-1″) and δ_H 5.47 (H-2″), and in HMBC spectrum, a long-range correlation was observed between δ_H 5.47 (H-2″) and δ_C 166.9 (C-7‴). Different from **2**, the HMBC correlation between δ_H [4.56 (1H, dd, *J* = 12.0, 4.0 Hz), 4.49 (1H, dd, *J* = 12.0, 2.0 Hz), H$_2$-6″] and δ_C 168.0 (C-7‴) was observed in **3**. On the basis of above-mentioned evidence, **2** and **3** were determined as 2,4′,6-trihydroxy-4-methoxybenzophenone-3-*C*-(2-*O*-*p*-hydroxybenzoyl)-*β*-D-glucopyranoside (**2**) and 2,4′,6-trihydroxy-4-methoxybenzophenone-3-*C*-(6-*O*-*p*-hydroxybenzoyl)-*β*-D-glucopyranoside (**3**), respectively.

Foliamangiferoside B (**4**) was isolated as a pale yellow powder and exhibited a positive optical rotation ($[\alpha]^{25}_D$ −3.5°, MeOH). The IR spectrum of **4** showed absorption bands at 3373, 1622, 1591, 1456, and 1705 cm^{-1} assignable to hydroxyl, aromatic ring, and carboxyl group. The molecular formula $C_{21}H_{24}O_{11}$ of **4** was determined by HR-Q-TOF-ESI-MS measurement with the positive-ion 445.1103 [M + Na]$^+$ and negative-ion *m*/*z* 421.1144 [M − H]$^-$. The ^{13}C NMR spectrum (Table 1) of **4** showed one more methoxyl group than that of compound **1**. The ^{1}H NMR (CD_3OD) spectrum and the ^{1}H−^{1}H COSY experiment on **4** indicated the presence of an ABX-system of aromatic protons

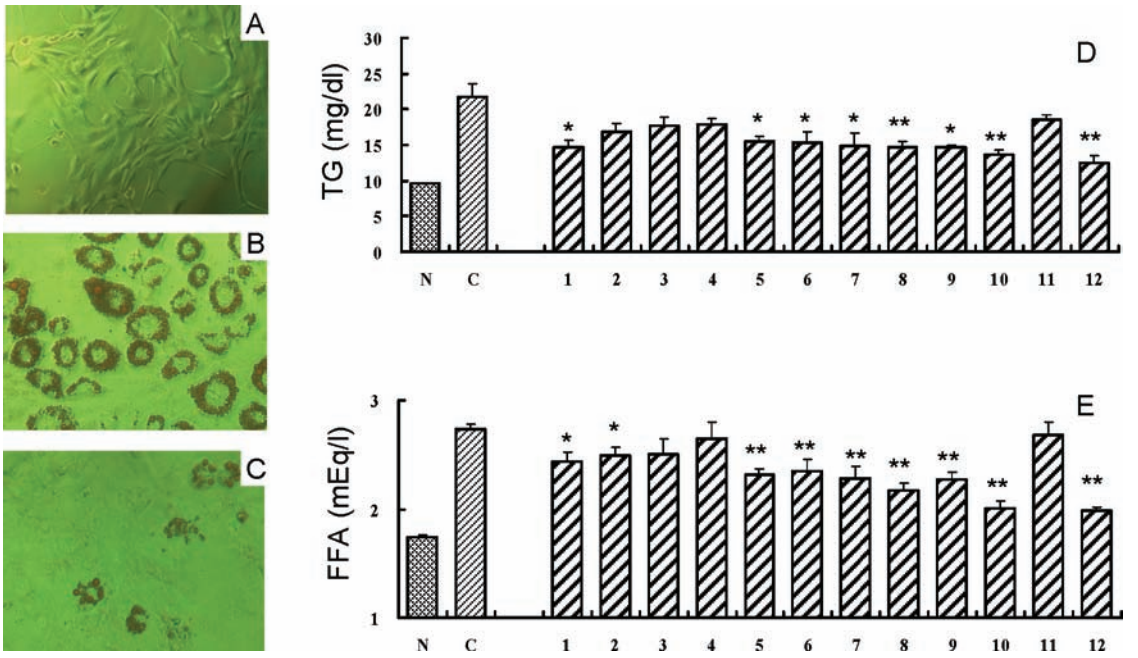

Figure 2. Cell images and TG and FFA levels in mature 3T3-L1 cells. Fourteen days after induction of differentiation, the cells were fixed and stained with Oil Red O. (A) Normal groups: cells were cultured without induction medium or any samples; no lipid droplets were observed (200×). (B) Control groups: cells were cultured with induction medium for 14 days; many lipid droplets were observed (100×). (C) Compound **10** treated groups: cells were cultured with induction medium and 30 μM compound **10**; little lipid droplets were observed (100×). Fourteen days after induction of differentiation, the cells were lysis by omni ruptor, respectively, and determined with the TG kit and NEFA kit according to the protocols provided by the manufacturer. (D) TG level in mature 3T3-L1 cells. (E) FFA level in mature 3T3-L1 cells. Values represent the mean ± SD of six determinations. *$P < 0.05$; **$P < 0.01$ vs control group. N: Normal group. C: Control group.

[δ 7.39 (1H, d, J = 2.0 Hz, H-2′), 7.28 (1H, dd, J = 2.0, 8.4 Hz, H-6′), and 6.78 (1H, d, J = 8.4 Hz, H-5′)], which were different from the AA′BB′-system of aromatic protons in compound **1**. The locations of hydroxyl, methoxyl group, carboxyl group, and glucosyl C−C linkage were clarified by HMBC correlation experiment and NOESY experiment shown in Figure 1. Consequently, the structure of foliamangiferoside B was characterized as 2,4′,6-trihydroxy-4,3′-dimethoxybenzophenone-3-β-D-glucopyranoside (**4**).

Foliamangiferoside C_1 (**5**) was obtained as a pale yellow amorphous powder with negative optical rotation ($[\alpha]^{25}_D$ −58.7°, MeOH). The molecular formula $C_{26}H_{24}O_{12}$ of **5** was measured on the basis of HR-Q-TOF-ESI-MS at m/z 527.1190 $[M - H]^-$ and 551.1151 $[M + Na]^+$. The ^1H (CD_3OD), ^{13}C (CD_3OD, Table 1), and various kinds of 2D NMR spectra indicated that there was a 2,4,4′,6-tetrahydroxybenzophenoneaglycon [δ_H 7.62 (2H, d, J = 8.4 Hz, H-2′,6′), 6.79 (2H, d, J = 8.4 Hz, H-3′,5′), 6.01 (1H, s, H-5); δ_C 198.9], a p-hydroxybenzoyl moiety [δ_H 7.85 (2H, d, J = 8.4 Hz, H-2‴,6‴), 6.79 (2H, d, J = 8.4 Hz, H-3‴,5‴); δ_C168.1], together with a C-β-D-glucopyranosyl moiety [δ_H 5.00 (1H, d, J = 10.0 Hz, H-1″); δ_C 79.5, 79.3, 76.6, 73.7, 71.2, 64.3]. In the HMBC experiment of **5**, long-range correlations were observed between δ_H 5.00 (H-1″) and δ_C 162.6 (C-4), 161.2 (C-2), and 104.2 (C-3); δ_H [4.62 (1H, dd, J = 12.0, 3.2 Hz), 4.53 (1H, br d, ca. J = 12 Hz), H_2-6″] and δ_C 168.1 (C-7‴); δ_H 7.85 (H-2‴,6‴) and δ_C 168.1 (C-7‴). Then the locations of the p-hydroxybenzoyl moiety and glucosyl C−C linkage were clarified. Consequently, foliamangiferoside C_1 was determined as 2,4,4′,6-tetrahydroxybenzophenone-3-C-(6-O-p-hydroxybenzoyl)-β-D-glucopyranoside (**5**).

Foliamangiferoside C_2 (**6**) was also obtained as a pale yellow amorphous powder with negative optical rotation ($[\alpha]^{25}_D$ −167.1°, MeOH). The molecular formula of **6** was determined as $C_{33}H_{28}O_{14}$ on the basis of HR-Q-TOF-ESI-MS at m/z 671.1381 $[M + Na]^+$ and 647.1427 $[M - H]^-$. The ^1H (CD_3OD), ^{13}C (CD_3OD, Table 1) of **6** showed one more p-hydroxybenzoyl moiety [δ_H 7.86 (2H, m, overlapped, H-2‴,6‴), 6.78 (2H, m, overlapped, H-3‴,5‴); δ_C 167.4 (C-7‴), 163.2 (C-4‴), 132.9 (C-2‴,6‴), 122.2 (C-1‴), and 116.2 (C-3‴,5‴)], than those of compound **5**. In the $^1H-^1H$ COSY spectrum (Figure 1), the $^1H-^1H$ correlations were observed between δ_H 5.27 (H-1″) and δ_H 5.59 (H-2″); δ_H 5.59 and δ_H 3.87 (H-3″); δ_H 3.87 and δ_H 3.78 (H-4″); δ_H 3.78 and δ_H 3.86 (H-5″); δ_H 3.86 and δ_H (4.66, 4.58, H_2-6″), and then the chemical shifts of all protons on sugar were determined. In the HMBC experiment (Figure 1), the following long-range correlations between proton and carbon were observed: δ_H 5.00 (H-1″) and δ_C 162.5 (C-4), 161.3 (C-2), 102.6 (C-3); δ_H 5.59 (H-2″) and δ_C 167.4 (C-7‴); δ_H [4.66, 4.58, H_2-6″] and δ_C 168.0 (C-7′‴). On the basis of above-mentioned evidence, the structure of foliamangiferoside C_2 was elucidated as 2,4,4′,6-tetrahydroxybenzophenone-3-C-[2,6-bis(O-p-hydroxybenzoyl)]-β-D-glucopyranoside (**6**).

Foliamangiferoside C_3 (**7**) was also obtained as a pale yellow amorphous powder with the molecular formula $C_{26}H_{24}O_{14}$, measured on the basis of HR-Q-TOF-ESI-MS at m/z 583.1059 $[M + Na]^+$ and 559.1109 $[M - H]^-$, which gave a negative optical rotation ($[\alpha]^{25}_D$: −23.0°, MeOH). The ^1H (CD_3OD), ^{13}C (CD_3OD, Table 1) spectra of **7** were superimposable on those of **5**, except for the signals due to a galloyl moiety [δ_H 7.09 (H-2‴,6‴); δ_C 168.4 (C-7‴), 146.4 (C-3‴,5‴), 139.8 (C-4‴), 121.2 (C-1‴), and 110.2 (C-2‴,6‴)]. The linkage of the galloyl moiety in **7** was also characterized by HMBC experiment, which showed long-range correlations between the 6″-proton [δ_C 4.58

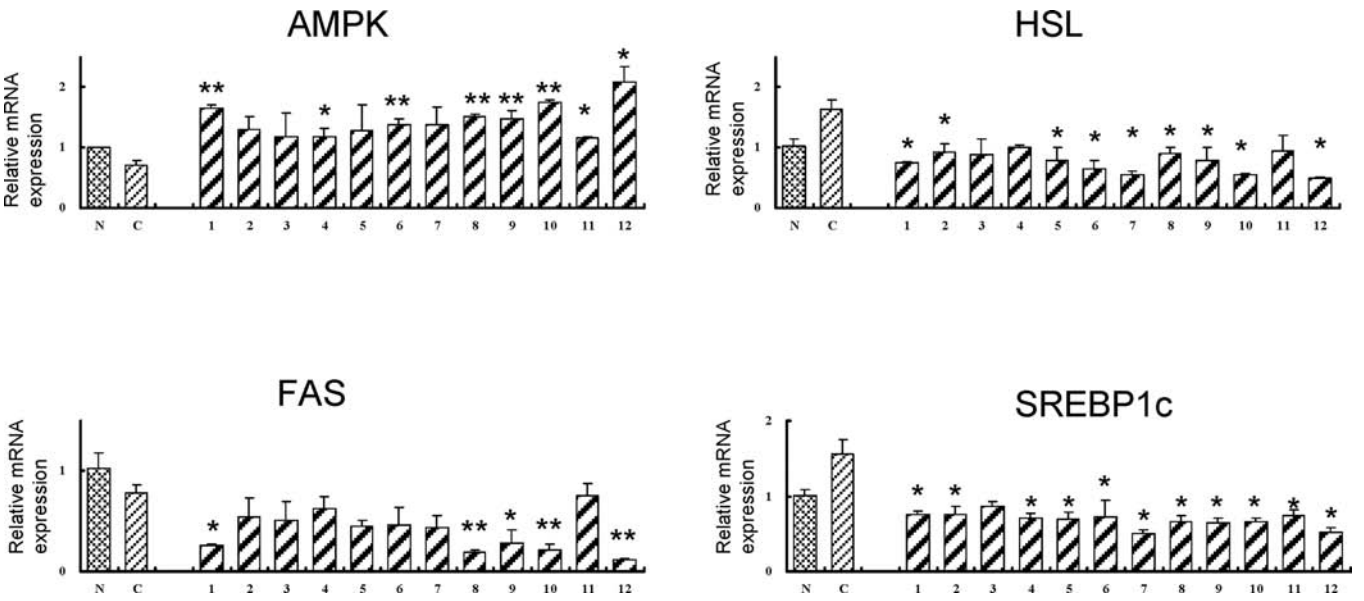

Figure 3. Effects of compounds **1**−**12** on AMPK, HSL, FAS, and SREBP1c mRNA expression level in mature 3T3-L1 cells. 3T3-L1 cells were incubated in induction medium with 30 μM compounds, respectively, for 14 days. Total RNAs were extracted to determine the mRNA levels. Values represent the mean ± SD of three determinations. Results were presented as levels of expression relative to those of controls after normalization to GADPH using the $2^{-\Delta\Delta CT}$ method. *$P < 0.05$; **$P < 0.01$ vs control group. N: Normal group. C: Control group.

(1H, dd, J = 12.0, 1.6 Hz), 4.46 (1H, dd, J = 12.0, 7.2 Hz)] and the 7‴-carbon (δ_C 168.4). Consequently, the structure of foliamangiferoside C_3 was elucidated to be 2,4,4′,6-tetrahydroxybenzophenone-3-*C*-(6-*O*-galloyl)-β-D-glucopyranoside (**7**).

Effect of Benzophenone *C*-Glucosides on TG and FFA Levels in Mature 3T3-L1 Cells. In the course of bioactive screening of Chinese natural medicines, we found that the 70% ethanolic extract of *M. indica* leaves had a strong inhibitory effect on TG accumulation in 3T3-L1 cells. This extract was partitioned in an EtOAc−H_2O (1:1, v/v) mixture to provide an EtOAc-soluble fraction and aqueous layer. The EtOAc fraction showed strong activity but the aqueous layer was weaker.

3T3-L1 preadipocytes were treated with the compounds **1**−**12** at doses of 30 μM. At this concentration, there were no treatment-related changes in cell viability. Fourteen days after the induction of differentiation in normal groups, wherein 3T3-L1 preadipocytes were cultured without induction medium or any sample, no significant lipid droplet was observed. In control groups, however, cells were cultured with induction medium for 14 days and many lipid droplets were observed (Figure 2).

As shown in Figure 2, compared to untreated cells, compounds **1**, **5**−**10**, and **12** significantly suppressed the accumulation of TG in mature 3T3-L1 cells, particularly mangiferin (**12**) whose inhibitory rate was 43.01 ± 0.14%. Ring C seco type compounds derived from **12**, such as compounds **1**, **8**, and **10**, inhibited TG accumulation less than that by compound **12** but no significant difference was found. This result indicated that the C-cycle of mangiferin is not an essential group in lipid metabolism. Compound **3** showed inhibitory effects weaker than that of **5**, suggesting that methylation of a 4-hydroxyl group reduces the inhibitory effect on TG accumulation. A similar structure−activity relationship was also observed in **9** and its 4-methylated compound, **2**. The free fatty acid content in mature 3T3-L1 cells was also determined, too. Compounds **1**, **2**, **5**−**10**, and **12** significantly suppressed the accumulation of FFA in mature 3T3-L1 cells. Compounds **10** and **12** presented the highest activity (inhibitory rates were 26.8 ± 2.7% and 27.5 ± 1.2%, respectively). As a result, the pattern of inhibitory effects on free fatty acid level was similar to that on TG accumulation (Figure 2).

AMPK plays an important role in regulating glucose, lipids, and cholesterol metabolism. When activated by conditions that deplete energy such as hypoxia, ischemia, and glucose deprivation, AMPK switches on catabolic pathways to generate ATP and to suppress ATP-consuming processes.[2] AMPK activation is known to decrease ACC activity and intracellular levels of malonyl CoA to further decrease the TG level and promote FFA oxidation.[18] In view of the changes in the TG and FFA level observed above, we hypothesized that this may be facilitated via activation of AMPK.

Compared with the normal group, AMPK gene expression in the control group was significantly down-regulated. Compared with the control group, AMPK gene expression of compounds **1**, **4**, **6**, and **8**−**12** were significantly increased.

We further investigated whether or not the above compounds regulate the expression level of adipogenic genes such as sterol regulatory element-binding protein 1c (SREBP1c), hormone-sensitive lipase (HSL), and fatty acid synthase (FAS). The results showed that all of these compounds, except **3**, significantly suppressed the SREBP1c level. Compounds **1**, **2**, **5**−**10**, and **12** significantly down-regulated HSL gene expression, and **1**, **8**−**10**, and **12** significantly reduced FAS gene expression (Figure 3).

We investigated the structure−activity relationship of benzophenone *C*-glucosides. Compared with mangiferin (**12**) and its C-ring cleavage type compound, **10**, no significant changes were found in the regulatory effects of AMPK, SREBP1c, HSL, and FAS gene expression, indicating that the C-ring is not the essential group. In the B-ring, 3′,4′-dihydroxyl-substituted compound showed virtually the same activity as compared with compound **8**, a B-ring 3′-hydroxyl-substituted type. However, the activity of the 3′-methoxy-4′-hydroxy type became more moderate than that of the mono- or dihydroxy type (**4** vs **1**, **8** and **10**).

Numerous studies have indicated that AMPK activation directly inhibits TG biosynthesis enzyme indirectly via suppression of SREBP1c.[19] SREBP1c is a critical transcription factor that stimulates several lipogenic enzymes involved in fatty acid biosynthesis. The above result indicated that the effects of compounds isolated from *M. indica* leaves significantly inhibited the expression of genes including SREBP1c, FAS, and HSL, all associated with TG biosynthesis. AMPK is activated by two distinct signals, a Ca^{2+}-dependent pathway mediated by CaMKKβ and an AMP-dependent pathway mediated by LKB1.[20] Associated with other upstream kinases, the AMPK α subunit was phosphorylated at Thr172. Binding AMP to the γ subunit leads to allosteric activation of AMPK as well as protection of Thr172 from dephosphorylation, thereby maintaining the enzyme in the activated state. Further studies on the effects of these compounds on the AMPK phosphorylate level are necessary.

AUTHOR INFORMATION

Corresponding Author

*Tel/Fax: 0086-22-5959-6163. E-mail: wangt@263.net.

Funding Sources

This research was supported by the Key Project of Chinese Ministry of Education. (No. 209002), Changjiang Scholars and Innovative Research Team in University (PCSIRT), Tianjin Committee of Science and Technology, China (10SYSYJC28900).

REFERENCES

(1) Schimmack, G.; Defronzo, R. A.; Musi, N. AMP-activated protein kinase: Role in metabolism and therapeutic implications. *Diabetes Obes. Metab.* **2006**, *8* (6), 591–602.

(2) Zhang, B. B.; Zhou, G.; Li, C. AMPK: an emerging drug target for diabetes and the metabolic syndrome. *Cell Metab.* **2009**, *9* (5), 407–16.

(3) Andreelli, F.; Foretz, M.; Knauf, C.; Cani, P. D.; Perrin, C.; Iglesias, M. A.; Pillot, B.; Bado, A.; Tronche, F.; Mithieux, G.; Vaulont, S.; Burcelin, R.; Viollet, B. Liver adenosine monophosphate-activated kinase-alpha2 catalytic subunit is a key target for the control of hepatic glucose production by adiponectin and leptin but not insulin. *Endocrinology* **2006**, *147* (5), 2432–41.

(4) Carey, A. L.; Steinberg, G. R.; Macaulay, S. L.; Thomas, W. G.; Holmes, A. G.; Ramm, G.; Prelovsek, O.; Hohnen-Behrens, C.; Watt, M. J.; James, D. E.; Kemp, B. E.; Pedersen, B. K.; Febbraio, M. A. Interleukin-6 increases insulin-stimulated glucose disposal in humans and glucose uptake and fatty acid oxidation in vitro via AMP-activated protein kinase. *Diabetes* **2006**, *55* (10), 2688–97.

(5) Hou, X.; Xu, S.; Maitland-Toolan, K. A.; Sato, K.; Jiang, B.; Ido, Y.; Lan, F.; Walsh, K.; Wierzbicki, M.; Verbeuren, T. J.; Cohen, R. A.; Zang, M. SIRT1 regulates hepatocyte lipid metabolism through activating AMP-activated protein kinase. *J. Biol. Chem.* **2008**, *283* (29), 20015–26.

(6) Zhang, F.; Sun, C.; Wu, J.; He, C.; Ge, X.; Huang, W.; Zou, Y.; Chen, X.; Qi, W.; Zhai, Q. Combretastatin A-4 activates AMP-activated protein kinase and improves glucose metabolism in db/db mice. *Pharmacol. Res.* **2008**, *57* (4), 318–23.

(7) JiangsuXinyixueyuan. *Dictionary of Traditional Chinese Medicines*; Shanghai Scientific and Technologic Press: Shanghai, 1977; p 199.

(8) Barreto, J. C.; Trevisan, M. T.; Hull, W. E.; Erben, G.; de Brito, E. S.; Pfundstein, B.; Wurtele, G.; Spiegelhalder, B.; Owen, R. W. Characterization and quantitation of polyphenolic compounds in bark, kernel, leaves, and peel of mango (*Mangifera indica* L.). *J. Agric. Food. Chem.* **2008**, *56* (14), 5599–610.

(9) Nong, C.; He, W.; Fleming, D.; Pan, L.; Huang, H. Capillary electrophoresis analysis of mangiferin extracted from Mangifera indica L. bark and Mangifera persiciformis C.Y. Wu et T.L. Ming leaves. *J. Chromatogr., B* **2005**, *826* (1−2), 226–31.

(10) Singh, U. P.; Singh, D. P.; Singh, M.; Maurya, S.; Srivastava, J. S.; Singh, R. B.; Singh, S. P. Characterization of phenolic compounds in some Indian mango cultivars. *Int. J. Food Sci. Nutr.* **2004**, *55* (2), 163–9.

(11) Aderibigbe, A. O.; Emudianughe, T. S.; Lawal, B. A. Evaluation of the antidiabetic action of Mangifera indica in mice. *Phytother. Res.* **2001**, *15* (5), 456–8.

(12) Severi, J. A.; Lima, Z. P.; Kushima, H.; Brito, A. R.; Santos, L. C.; Vilegas, W.; Hiruma-Lima, C. A. Polyphenols with antiulcerogenic action from aqueous decoction of mango leaves (Mangifera indica L.). *Molecules* **2009**, *14* (3), 1098–110.

(13) Nkuo-Akenji, T.; Ndip, R.; McThomas, A.; Fru, E. C. Anti-Salmonella activity of medicinal plants from Cameroon. *Cent. Afr. J. Med.* **2001**, *47* (6), 155–8.

(14) Ge, D.; Zhang, Y.; Liu, E.; Wang, T.; Hu, L. Chemical constituents of Mangifera indica leaves (I). *Zhongcaoyao* **2011**, *42* (3), 428–31.

(15) Pinent, M.; Blade, M. C.; Salvado, M. J.; Arola, L.; Ardevol, A. Intracellular mediators of procyanidin-induced lipolysis in 3T3-L1 adipocytes. *J. Agric. Food. Chem.* **2005**, *53* (2), 262–6.

(16) Livak, K. J.; Schmittgen, T. D. Analysis of relative gene expression data using real-time quantitative PCR and the 2(T)(-Delta Delta C) method. *Methods* **2001**, *25* (4), 402–408.

(17) Tanaka, T.; Sueyasu, T.; Nonaka, G.; Nishioka, I. Tannins and Related Compounds. XXI. Isolation and Characterization of Galloyl and p-Hydroxybenzoyl Esters of Benzophenone and Xanthone C-Glucosides from Mangifera indica L. *Chem. Pharm. Bull.* **1984**, *32* (7), 2676–2686.

(18) McCarty, M. F. AMPK activation as a strategy for reversing the endothelial lipotoxicity underlying the increased vascular risk associated with insulin resistance syndrome. *Med. Hypotheses* **2005**, *64* (6), 1211–1215.

(19) Kohjima, M.; Higuchi, N.; Kato, M.; Kotoh, K.; Yoshimoto, T.; Fujino, T.; Yada, M.; Yada, R.; Harada, N.; Enjoji, M.; Takayanagi, R.; Nakamuta, M. SREBP-1c, regulated by the insulin and AMPK signaling pathways, plays a role in nonalcoholic fatty liver disease. *Int. J. Mol. Med.* **2008**, *21* (4), 507–11.

(20) Sanders, M. J.; Grondin, P. O.; Hegarty, B. D.; Snowden, M. A.; Carling, D. Investigating the mechanism for AMP activation of the AMP-activated protein kinase cascade. *Biochem. J.* **2007**, *403* (1), 139–48.